Silica supported phosphine gold complexes as an efficient catalytic system for a dearomative spirocyclization

Zhen Cao, Antoine Scalabre, Sylvain Nlate, Sonia Buffiere, Reiko Oda, Emilie Pouget, Brigitte Bibal

Silica supported phosphine gold complexes as an efficient catalytic system for a dearomative spirocyclization

Zhen Cao,[a] Antoine Scalabre,[b] Sylvain Nlate,[b] Sonia Buffière,[c] Reiko Oda,[b] Emilie Pouget,*[b] and Brigitte Bibal*[a]

[a] Z. Cao, Dr B. Bibal*
Institut des Sciences Moléculaires, UMR CNRS 5255
Université de Bordeaux
351 cours de la Libération, 33405 Talence, France
E-mail: brigitte.bibal@u-bordeaux.fr

[b] Dr A. Scalabre, Dr S. Nlate, Dr R. Oda, Dr E. Pouget*
Chimie et Biologie des Membranes et des Nanoobjets, UMR CNRS 5248
Université de Bordeaux
2 rue Roger Escarpit, 33607 Pessac, France
E-mail: : e.pouget@cbmn.u-bordeaux.fr

[c] S. Buffière
Institut de Chimie de la Matière Condensée de Bordeaux, UMR CNRS 5026
Université de Bordeaux
87 avenue du docteur Schweitzer, 33608 Pessac, France

Supporting information for this article is given via a link at the end of the document.

Abstract: The combination of metal catalyst and inorganic silica frames provides a greener approach for recyclable catalysis. Herein, chiral silica nanohelices were successfully employed to covalently graft three phosphine gold chloride complexes. The resulting 3D ensembles showed chiroptical properties that allowed the monitoring of the supported ligands. The heterogeneous gold chloride catalysts in cooperation with silver triflate exhibited a high reactivity in various reactions, especially for the spirocyclization of aryl alkynoate esters when a catalytic loading of 0.05 %mol can be employed. The heterogeneous catalysts were easily recovered and can be recycled up to 7-8 times without any loss of efficiency. By adding more silver triflate, 25 cycles with full conversion can be reached, due to a more complex catalytic system based on silica and metallic species.

Introduction

Immobilization of metallic complexes onto a solid support has attracted considerable attention in synthetic chemistry as it offers removable catalysts with facile product purification.[1] Compared to the homogeneous conditions, the recyclability and reusability of the supported catalysts provide waste-reduced and greener processes.

In the field of gold catalysis,[2] phosphine and *N*-heterocyclic carbene gold complexes have been supported at the surface or embedded in organic polymers,[3] zeolites or silica (FDU-12, SBA, MCM-41)[4], and they successfully reproduced the efficiency and enantioselectivity reported for the related homogeneous systems (Fig. 1).[5] Interestingly, many heterogeneous catalysts exhibited a variable recyclability of four to eight cycles on average, with acceptable yields (90-99%) and reaction times (24h). Such supported gold complexes have also been presented as an efficient alternative to the well-known deactivation of the cationic gold(I) catalysis[6] observed under homogeneous conditions. The main pathways of this decay have been identified as silver effects,[7] the gold reduction triggered by reductants[8] in the reaction system (such as water), and a possible disproportionation[9] induced by the substrate. However, a few studies encompassed the deactivation of gold catalysts when recycling heterogeneous catalysts over extended times.[4e,10] Among those reported so far, the use of porous supports is proposed to improve catalysis by a better contact between catalysts and hydrophobic reactants in mesoporous polymers.[3g] The acidity of the silica supports is also suggested as a possible assistance for catalysis (Fig. 1).[4b,4c] Due to the fragility of cationic gold(I), the nature of the catalytic species with a long-term recyclability is still questionable in the case of supported gold complexes.

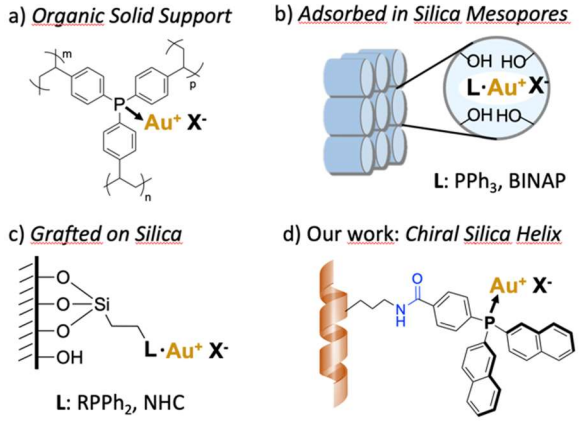

Figure 1. Main strategies for supporting gold complexes in heterogeneous catalysis: a) insertion in an organic (porous) polymer; b) adsorption on silica mesopores to benefit from an acidic assistance, c) covalent grafting on silica particles or mesoporous silica and d) our work: grafting on a chiral silica nanohelix to form a chiroptical ensemble for a long-term monitoring.

Previously, we reported the fabrication of silica nano-helices based on sol-gel transcription of molecular self-assembly whose handedness (Plus or Minus for the right- and left- handed helices respectively), morphology and size can be controlled.[11] Recently, these nano-objects were employed as inorganic supports for discrete species of different sizes: (i) 5–10 nm gold nanoparticles[12] that organize into 3D helical superstructures, (ii) large polyoxometalate (POM) clusters[13] that catalyse the oxidation of thioethers, and (iii) grafted organic dyes (pyrene and perylenediimide derivatives)[14]. For all these cases, it was clearly shown that the grafted moieties present induced CD signals. Based on these results, we anticipate that a silica nanohelix can also act as a robust support for molecular metal catalysts, such as triphenylphosphine gold chloride complex PPh_3AuCl, leading to a 3D ensemble with additional chiroptical[15] properties useful for monitoring the life cycle of supported ligands. To date, the behavior of metallic catalysts on chiral silica nano-objects has never been investigated.

Herein, we report a series of heterogeneous gold(I) complexes based on arylphosphine ligands covalently linked to chiral silica supports for catalysis. Three model phosphine ligands were designed as chromophores capable to conjugate with the silica material by peptide coupling (Scheme 1): tris-phenyl derivative **L1**, dinaphthyl **L2** and tris-phenyl ligand with an alkyl spacer **L3** to evaluate any effect of the spacer length. In addition, two types of silica objects were tested as supports: non-chiral spherical nanoparticles (Si-NP, diameter: 52 nm) and chiral nano-helices (diameter: 37 nm) that have larger specific surfaces: 50 m^2/g for Si-NP and 170 m^2/g for helices.

The Lewis acid properties of the new immobilized gold(I) phosphine complexes were evaluated towards substituted alkynes leading to four different products, including a spirocyclization of anisole derivatives. In addition, the nature of the catalytic system along recycling was monitored.

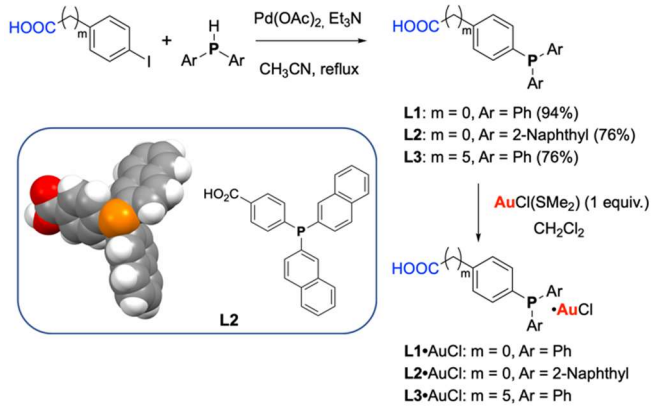

Scheme 1. Synthesis of phosphine-gold chloride complexes **Ln·AuCl** (n = 1–3) bearing a carboxylic group for grafting on silica nanoparticles and helices functionalized with amines. Inset: crystallographic structure of ligand **L2** (CCDC number 2006391).

Results and Discussion

Preparation of grafted gold complexes

Ligand **L1** was prepared according to literature[16] and new phosphines **L2**–**L3** were synthetized via a key C(sp^2)-P coupling catalyzed by palladium between an aryliodide and a diarylphosphine (76% yield, scheme 1). The crystallographic structure of **L2** revealed that the phosphorus atom is still available for metal coordination, even provided with bulky substituents such as 2-naphthyl ones (see Supporting Information, SI). The corresponding gold chloride complexes **Ln·AuCl** (n = 1–3) were obtained in excellent yield (85-95% yield) by mixing each phosphine ligand with one equivalent of $AuCl(SMe_2)$.

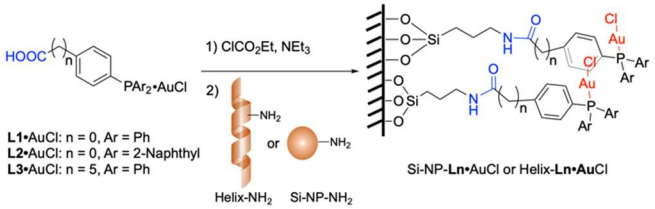

Figure 2. A peptide coupling allows the covalent grafting of gold complexes on silica nanoparticles and helices to get heterogeneous catalysts Si-NP and helix-**Ln·AuCl** (n = 1–3).

The robust anchoring of gold complexes to silica was ensured by a peptide coupling under smooth conditions (ethyl chloroformate, Et_3N, dry acetone, 0–20°C)[14] between gold complexes **Ln·AuCl** (n = 1–3) and silica NP or helices functionalized by amines (Fig. 2, Si-NP-NH_2 and Helix-NH_2 respectively). It should be noted that the coupling of phosphines **Ln** (non coordinated ligands) to the support rapidly led to the phosphine oxidation which prevents their subsequent use for the coordination of gold atoms (see SI). All grafted silica materials *i.e.* NP-**Ln·AuCl** and Helix-**Ln·AuCl** were insoluble in organic solvents, making them prime candidates for heterogeneous gold catalysis.

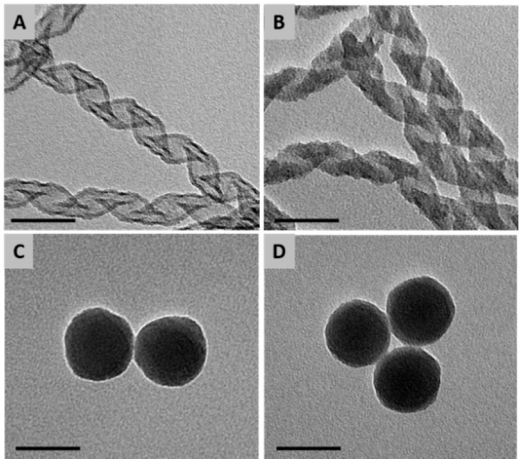

Figure 3. TEM images of P-Helix-NH_2 before grafting (A), P-Helix-**L2·AuCl** after grafting (B), Si-NP-NH_2 before grafting (C) and Si-NP-**L2·AuCl** after grafting (D). Scale bar: 50 nm.

Analysis by transmission electron microscopy (TEM) of silica materials before and after the grafting of gold complexes indicated a homogeneous darkening of the helices due to the presence of phosphine gold complexes (Fig. 3 A-B) meanwhile no difference can be visualized for nanoparticles (Fig. 3 C-D) because of their higher silica tickness inducing a denser material to the electrons than the helices. Even if the thin layer of gold complex on Si-NP cannot change the contrast in TEM analysis, the grafting of gold complexes on nanoparticles has been confirmed by energy dispersive spectroscopy (EDS, see SI).
The atomic percentage of gold (*versus* silicon) for these new organic-inorganic materials was obtained by EDS for all samples (see SI): 0.3 ± 0.1 % for NP-**Ln·AuCl** and 0.9 ± 0.2 % for Helix-**Ln·AuCl** with very good reproducibility for several (3 to 8) samples. The measured gold density on the silica surface was 0.5 Au/nm² for the helices and 0.6 Au/nm² for the NPs based on their specific surfaces (see SI). Knowing that the amine density on silica is generally comprised between 0.7 and 1 amine per nm²,[12] it can be considered that the maximum loading of gold complexes is reached. The gold complex grafting on both silica NP and helices is then high, homogeneous and reproducible.
In the case of the helices, the chirality induction from the silica helices to the grafted ligands was revealed by circular dichroism (CD) spectroscopy (Fig. 4). Opposite CD signals for P- and M- Helix-**Ln·AuCl** (n = 1–3) were observed in the 210-330 nm region, corresponding to the absorbance of the aryl groups belonging to the ligands. The CD spectra indicated little impact from the alkyl spacer (m = 0, 5) between the ligand and the nano-objects, when comparing silica materials grafted with **L1·AuCl** and **L3·AuCl**.

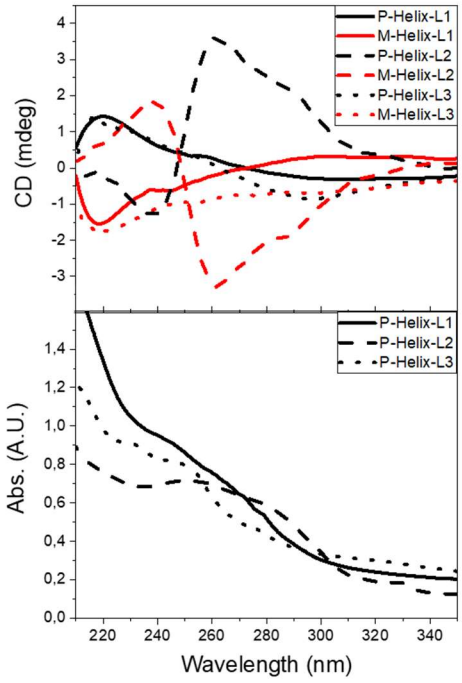

Figure 4. Representative spectrum of circular dichroism (CD) and UV-Visible spectroscopy for P- (black) and M- (red) Helix-**Ln·AuCl** (n = 1–3) in ethanol (500 μg/mL).

As expected from the ligands design, enhanced CD signals are observed for Helix-**L2·AuCl** due to its naphthyl substituents (*versus* phenyl ones for Helix-**Ln·AuCl**, n = 1, 3) which probably participate to the molecular coupling via extended π-stacking, inducing a Cotton effect. Such a phenomenon of chiral induction has already been observed when large partners (AuNP, POM)[12-13] and organic polyaromatic compounds (pyrene and perylenediimide)[14] were associated to helices. The origin of this observation is still under investigation.
Finally, a homogeneous and reproducible covalent grafting of the gold complexes onto silica nanoparticles and helices can be assumed from combined TEM, EDS and CD analyses of samples.

Heterogeneous gold catalysis

The Lewis acid activity of the supported cationic gold complexes was evaluated upon three classical alkyne activations using Helix-**L2·AuCl** as a model catalyst (2 mol%) in the presence of silver triflate as a chloride scavenger (6 mol%) in dichloromethane at room temperature over 24h (Scheme 2). Under heterogeneous conditions, the cyclization of the propargylic amide afforded a mixture of the 5-*exo*-dig product and its oxazole isomer in a (2:1) ratio (70% conv., Scheme 2a). This activity is similar to other gold complexes under homogeneous conditions (79% conv., 36h).[17] The supported complex was also effective for the cyclization of 1,6-enyne[18] into the 5-*exo-dig* product, *i.e*. a vinyl cyclopentene (100% conv., Scheme 2b) and the hydration of 1-phenylprop-2-ynylacetate[19] (99% yield, Scheme 2c), with reaction times of 24h. The three model reactions were similarly catalyzed by gold complexes under homogeneous and helix-supported conditions.

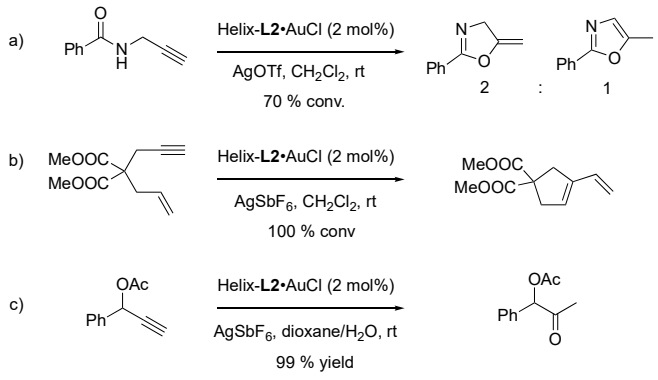

Scheme 2. Alkyne activation under heterogeneous conditions over 24h using Helix-**L2·AuCl** (2 mol%) as a catalyst for the transformation of : a) a propargylic amide into the 5-*exo*-*dig* product and its oxazole isomer in a (2:1) ratio; b) a 1,6-enyne into the 5-*exo*-*dig* product; c) an terminal alkyne into a ketone by water addition.

To further investigate the catalytic activity of the supported gold complexes, the dearomative spirocyclization of aryl alkynoate esters **S1** and **S2** was selected as a benchmark reaction (Table 1). Under homogeneous conditions, Vadola *et al*. showed that Ph_3PAuCl (5 mol%) and AgOTf (5 mol%) catalyzed the reaction in dichloromethane, in the presence of water (1 equiv.) that assists the demethylation step.[20, 21] The transformation of **S1** is described as rapid (90% yield, 30 min) and it was reproduced under slightly different conditions (90% yield, 12h, Table 1, entry 1). In our hands, the process was found to be concentration dependent, requiring at least a concentration of 50 mM in substrate to observe any conversion of **S1**.

By employing gold chloride complexes supported on silica NP and helices (3-10 mol%) and silver triflate[22] (30 mol%) as the catalytic system, the reaction proceeds smoothly with alkynes **S1** and **S2** (Table 1, entries 2-7) in 99% conversion into the corresponding spirocycles. As expected, the difference in the silica morphology (NP *versus* Helix) and the catalyst loading (3-10 mol%) do not have a detectable impact on the activity of the supported gold complexes.

As the silica helix support is chiral, the enantiomeric ratio of spirocycles obtained in the presence of gold catalysts supported on P- and M- helices was analyzed by chiral HPLC (see SI). No chiral induction from enantiopure Helix-**L2·AuCl** to the molecular scale (spirocycles) chirality was observed (*i.e*. no detectable enantiomeric excess). This result is expected for such a "large scale" chiral ensemble (over 100 nm), as asymmetric catalysis is reported for homogeneous gold complexes provided by bulky chiral ligands that impact on the coordinated substrate.[23]

To assess the catalytic role of gold, control experiments were carried out. A silica nanoparticle NP-NH_2 without any gold complex cannot catalyze the reaction (Table 1, entry 8). The direct acidic catalysis from the silica surface is then dismissed. Besides, the silver triflate alone does not catalyse this reaction, even after 48h (Table 1, entry 9). Interestingly, the reaction is slowly achieved by the combination of Si-NH_2 nanoparticle and silver triflate, in the presence of water and can reach 16% conversion after 24h (66 % yield after 6 days) which suggests the generation of silver nanoparticles. As reported by Taylor and Unsworth,[24] aged silver nitrate salts in the presence of silica can catalyze similar spirocyclisations. Nonetheless this secondary catalytic activity of AgOTf with silica is marginal compared to the one observed with supported cationic gold complexes, with short reaction times (5–24h) such as used in this study.

Finally, the catalyst loading was optimized for Helix-**L2·AuCl** towards the dearomative *ipso*-cyclization reaction of **S2** (Table 1, entries 11-13). The reaction was achieved with a catalytic loading as low as 0.05 mol% in 16 h with an excellent yield of 97% (Table 1, entry 13). This result is remarkable compared to those obtained with other supported gold complexes[3–5] that were typically efficient in a range of 1-10 mol% for different reactions over a maximum of 24h. This efficiency at low loading could be attributed to our strategy of catalyst preparation in which pure gold-phosphine complexes were grafted on the acidic supports which is an opposite strategy compared to the literature (grafting of ligand followed by coordination)[25].

Table 1. Dearomative spirocyclization of aryl alkynoate esters **S1**–**2** catalyzed by gold complexes grafted on silica nano-objects. [a]

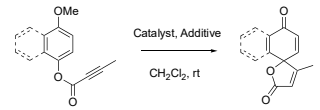

Benzene derivative **S1**
Naphthalene derivative **S2**

Spirocycles

Entry	Substrate	Catalyst	Catalytic loading	Additive	Reaction time	Yield[c]
1[b]	S1	PPh_3AuCl	10 mol%	AgOTf	12 h	99 % (90 %)[d]
2	S1	NP-L1·AuCl	3 mol%	AgOTf	5 h	99 %
3	S2	NP -L2·AuCl	3 mol%	AgOTf	5 h	99 %
4	S2	NP -L3·AuCl	1.5 mol%	AgOTf	24 h	99 %
5	S1	Helix-L1·AuCl	5 mol%	AgOTf	16 h	99 %
6	S2	Helix-L2·AuCl	10 mol%	AgOTf	5 h	99 %
7	S1	Helix-L3·AuCl	5 mol%	AgOTf	16 h	99 %
8	S1	NP-NH_2	10 mol%[e]	-	3 days	Trace
9	S1	AgOTf	30 mol%	-	2 days	Trace
10	S1	NP-NH_2	10 mol%[e]	AgOTf	24 h	16%[f]
11	S2	Helix-L2·AuCl	1 mol%	AgOTf	24 h	99 %

12	S2	Helix-L2·AuCl	0.1 mol%	AgOTf	24 h	99 %
13	S2	Helix-L2·AuCl	0.05 mol%	AgOTf	16 h	99 % (97 %)[d]

[a] Standard procedure: the reaction was performed by stirring substrate **S1** or **S2** (0.04 mmol), H_2O (10 μL), the gold chloride catalyst (10 mol%) and AgOTf (30 mol%) in CH_2Cl_2 (3 mL) at room temperature in aluminium foil. [b] Under homogeneous conditions, the reaction appeared to be dependent on substrate concentration, requiring at least 50 mM. [c] Conversion was determined by ^{1}H NMR. [d] Isolated yield. [e] Calculated for available amine groups. [f] Conversion reached 66% after 6 days.

Recyclability of catalysts

In order to take advantage of its heterogeneous nature, the recyclability of silica-supported gold complexes was investigated for the dearomative spirocyclization of substrates **S1-2**. NP-**Ln·AuCl** catalysts were partially recovered during recycling processes that employ washings with dichloromethane. As a consequence, gold catalysts supported on NPs were not considered for the following recycling experiments.

The recyclability of silica-supported Helix-**Ln·AuCl** catalysts (n = 1–2) was examinated with an initial loading of 10 mol%. During the recyclability process, each Helix-**Ln·AuCl** catalyst was readily recovered simply by centrifugation after the reaction completion (monitored by TLC and ^{1}H NMR) and it was used for next catalytic cycle without any further treatment. For all supported catalysts (Fig. 5 and Fig. S10), full conversion was reached at each cycle, with reaction times gradually increasing from 5h (initial cycle) to 24h at the seventh cycle. Thus, in order to continue the catalytic cycles, an additional portion of AgOTf (30 mol%) should be added every 7 cycles. This experiment was followed over to 25 cycles with full conversions. Compared to homogeneous cationic gold complexes that rapidly deactivate over 24h-48h and cannot be refreshed by silver salts, the long-living behaviour of these supported gold complexes with an additional silver assistance require further investigation.

The nature of the silica supported catalysts was examined after four cycles by TEM, EDS and CD spectroscopy (see Fig. 6 and SI). The CD signals obtained from the phosphine ligand grafted to silica are comparable before and after the cycles of reactions. Notably, the UV-Visible spectra presented a broad absorbance in the 400-500 nm region, which is characteristic of the presence of AgNPs in contrast with AuNPs that absorb in the 500-600 nm region.[26] Besides, TEM images indicated the presence of small nanoparticles (~3 nm) on the surface of the helices and larger aggregates (~100-500 nm) in the medium (Fig. 6 A-C), which metal composition has to be clarified. Finally, the EDS analysis of this recycled catalytic material revealed the main presence of silver (1.7 ± 0.6 %), forming large aggregates (100-500 nm, Fig. 6 D) and a large decrease in gold content (0.9% after preparation *versus* 0.1% after 4th cycle).

Metal leaching from the silica support is a classical phenomenon for most immobilized metallic complexes. Indeed, J. A. Gladysz and V. Farina already pointed their limited efficiency over cycles and metal leaching that questionned their economic benefits *versus* their cost of preparation.[27] In the case of gold complexes, an additional question arises from the nature of the catalytic species.

Based on these analyses, the recycled material appeared to gradually transform over time and cycles, with a decrease in cationic gold(I) catalysts and the possible presence of Ag(I)-SiO_2 catalytic species,[24] as the catalytic activity is instantly boosted by the addition of AgOTf after seven cycles. The *in situ* reduction of gold(I) and Ag(I) into nanoparticles also accounts for the observed increase in reaction times, and reveals uncontrolled pathways of the catalyts deactivation. The exact nature of catalytic species is still under investigation in our laboratory. In a more general view, our report is questioning previous examples of supported gold complexes, even embedding ones, that are recycled over 5-8 runs. A plausible catalytic activity emerging from supported Ag(I) or AgNP should be carefully taken into account.

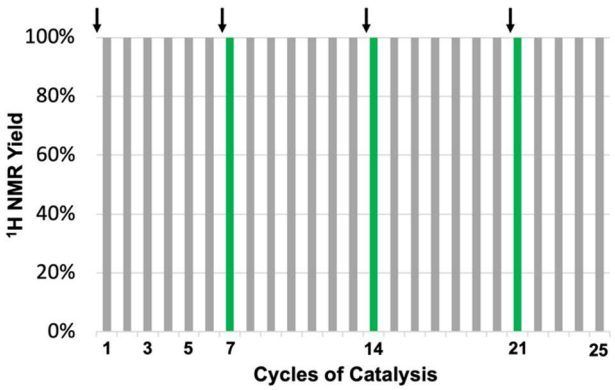

Figure 5. Recyclability of Helix–**L1·AuCl** catalyst (10 mol%) for the spirocyclization of substrate **S1** over 25 cycles. In this case, reasonnable reaction times (ca. 24h max) are maintained by adding AgOTf (30 mol%) every 7th cycle (black arrow).

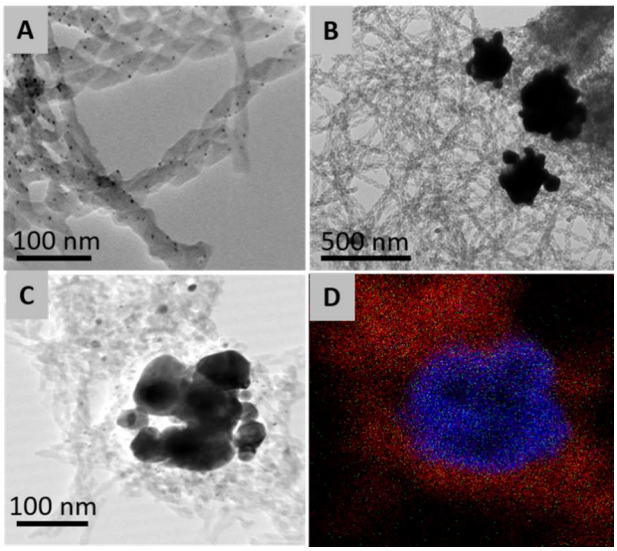

Figure 6. TEM images of Helix–**L2·AuCl** after four catalytic cycles showing the still presence of helices and the apparition of small (A) and larger (B and STEM image C) particles. The EDS mapping (D) shows that the particles are silver (red is silicon and blue is silver).

Conclusion

Two new phosphine ligands **L2–3** were designed for conjugation through peptide coupling. Metallic catalysts i.e. gold chloride phosphines were successfully grafted to silica by directly linking to the support avoiding any phosphine oxidation. The chiroptical properties of these supported gold complexes were exploited by monitoring the ligand linkage to the support. We highlighted that the combination of the inorganic silica nano-objects and gold complexes provides an efficient green approach for several types of alkynes cyclizations. More importantly, the heterogeneous catalysts could be recycled up to an average 7 cycles without any loss of efficiency in the dearomative spirocyclization reaction of aryl alkynoate esters. The catalytic system can be boosted by adding silver triflate. Interestingly, the supported cationic gold(I) catalysts appeared to gradually be transformed over time and recycling cycles, but the catalytic system exhibited a remarkable long-lasting activity. Further investigations will focus on the characterization of the catalytically active silica and metallic species.

Experimental Section

General procedure for the synthesis of gold complexes. To a solution of ligand **L1–3** (1.0 equiv) in dry dichloromethane (1 mL) was added a solution of $AuCl(SMe_2)$ (1.0 equiv) in dichloromethane (0.5 mL) under argon at room temperature. After stirring for 5 h, the solution was concentrated to *ca.* 0.3 mL and diethyl ether (1.5 mL) was added. After stirring for 5 min, the white solid was filtered and dried under vacuum to give the corresponding **Ln·AuCl** complex (n = 1–3).

General procedure for grafting gold complexes onto silica nano-objects. To a solution of **Ln·AuCl** complex (n = 1–3, 5~10 mg, 0.013-0.015 mmol) in acetone (4 mL, dried over activated 4 Å MS) were added triethylamine (30 µL, 0.21 mmol) and ethyl chloroformate (20 µL, 0.21 mmol) under argon atmosphere at 0°C. The mixture was stirred at 0°C for 30 min then allowed to warm up to room temperature. After 2 h, the mixture was added to a suspension of the amino-silica material (P– or M– Helix-NH_2 or Si-NP-NH_2) (1~3 mg) in dry acetone (2 mL) placed in 15 mL plastic tube. The resulting mixture was stirred for 16 h. After the addition of acetone (5 mL), the mixture was centrifugated at a speed of 3900 g for 20 min to get the suspension of gold complex grafted on silica material (L/D Helix-**Ln·AuCl** or NP-**Ln·AuCl**, n = 1–3) in acetone. After removing the supernatant, the resulting gel was washed with dry dichloromethane (3×10 mL).

General procedure for the dearomative *ipso*-cyclization reaction. To a suspension of supported gold complex (5-10 mol%, P– or M– Helix-**Ln·AuCl** or NP-**Ln·AuCl**, n = 1–3) in dry dichloromethane (2 mL) placed in a sealed glass tube was added silver triflate (0.01 mmol, 30 mol%). The mixture was stirred at room temperature for 30 min forming a brown suspension. Substrate S1–2 (0.04 mmol) and water (10 µL) were successively added. The resulting mixture was stirred for 5-24 h.

General procedure for catalyst recyclability. After the completion of the first cycle according to the general procedure, the crude system was centrifuged at 3900 g and washed with dry dichloromethane for three times. The conversion was monitored by ^1H NMR. The recovered supported material was dispersed again in dry dichloromethane (2 mL) for the next catalytic cycle.

Acknowledgements

Financial support was provided by the China Scholarship Council (Z.C. fellowship), Agence Nationale pour la Recherche (ANR-CONACYT-159884), the University of Bordeaux, and the Centre National de la Recherche Scientifique (CNRS). The authors thank Aline Lacoudre (CESAMO, Université de Bordeaux) for the structural resolution of ligand L2 by X-ray crystallography and the Placamat platform for the TEM characterizations.

Keywords: gold complex • heterogeneous catalysis • silica nanohelices • spirocyclization • circular dichroism

[1] a) C. A. McNamara, M. J. Dixon, M. Bradley, *Chem. Rev*., **2002**, *102*, 3275-3300; b) A. Corma, H. Garcia, *Adv. Synth. Catal*., **2006**, *348*, 1391-1412; c) M. B. Gawande, P. S. Branco, R. S. Varma, *Chem. Soc. Rev*., **2013**, *42*, 3371-3393; d) S. Fukuzumi, Y.-M. Lee, W. Nam, *ChemCatChem*, **2018**, *10*, 1686-1702.

[2] For selected reviews about homogeneous gold catalysis based on Lewis acidity, see: a) D. J. Gorin, F. D. Toste, *Nature*, **2007**, *446*, 395−403; b) A. S. K. Hashmi, *Chem. Rev.*, **2007**, *107*, 3180−3211; c) T. C. Boorman, I. Larrosa, *Chem. Soc. Rev.*, **2011**, *40*, 1910−1925; d) B. Ranieri, I. Escofet, A. M. Echavarren, *Org. Biomol. Chem.*, **2015**, *13*, 7103-7118; e) W. Zi, F. D. Toste, *Chem. Soc. Rev.*, **2016**, *45*, 4567−4589.

[3] a) M. Raducan, C. Rodriguez-Escrich, X. C. Cambiero, E. C. Escudero-Adan, M. A. Pericas, A. M. Echavarren, *Chem. Commun*., **2011**, *47*, 4893-4895; b) W. Cao, B. Yu, *Adv. Synth. Catal.*, **2011**, *353*, 1903-1907; c) M. Egi, K. Azechi, S. Akai, *Adv. Synth. Catal*., **2011**, *353*, 287-290; d) M. Chen, Z.-M. Zhang, Z. Yu, H. Qiu, B. Ma, H.-H. Wu, J. Zhang, *ACS Catal*., **2015**, *5*, 7488-7492; e) R. Cai, X. Ye, Q. Sun, Q. He, Y. He, S. Ma, X. Shi, *ACS Catal*., **2017**, *7*, 1087-1092; f) S. Tsupova, A. Cadu, S. A. C. Carabineiro, M. Rudolph, A. S. K. Hashmi, *J. Catal.*, **2017**, *350*, 97-102; g) H. Gu, X. Sun, Y. Wang, H. Wu, P. Wu, *RSC Adv.*, **2018**, *8*, 1737-1743.

[4] a) A. Corma, E. Gutierrez-Puebla, M. Iglesias, A. Monge, S. Perez-Ferreras, F. Sanchez, *Adv. Synth. Catal.*, **2006**, *348*, 1899-1907; b) G. Villaverde, A. Corma, M. Iglesias, F. Sanchez, *ACS Catal.*, **2012**, *2*, 399-406; c) X. Z. Shu, S. C. Nguyen, Y. He, F. Oba, Q. Zhang, C. Canlas, G. A. Somorjai, A. P. Alivisatos, F. D. Toste, *J. Am. Chem. Soc.*, **2015**, *137*, 7083-7086; d) Q. Nie, F. Y. Yi, B. Huang, M. Z. Cai, *Adv. Synth. Catal.*, **2017**, *359*, 3968-3976; e) J. T. Sarmiento, S. Suarez-Pantiga, A. Olmos, T . Varea, G. Asensio, *ACS Catal*., **2017**, *7*, 7146-7155; f) W. Yang, L. Wei, T. Yan, M. Cai, *Catal. Sci. Technol.*, **2017**, *7*, 1744-1755.

[5] For alternative strategies of gold complexes heterogenization, see: a) L. Liu, X. Zhang, J. Gao, C. Xu, *Green Chem.*, **2012**, *14*, 1710-1720; b) C. Vriamont, M. Devillers, O. Riant, S. Hermans, *Chem.–Eur. J*., **2013**, *19*, 12009-12017; c) J. Vaclavik, M. Servalli, C. Lothschütz, J. Szlachetko, M. Ranocchiari, J. A. van Bokhoven, *ChemCatChem*, **2013**, *5*, 692-696; d) D. Hueber, M. Hoffmann, P. de Frémont, P. Pale ,A. Blanc, *Organometallics*, **2015**, *34*, 5065-5072; e) M. Mon, J. Ferrando-Doria, T. Grancha, F. R. Fortea-Pérez, J. Gascon, A. Leyva-Pérez, D. Armentano, E. Pardo, *J. Am. Chem. Soc.*, **2016**, *138*, 7864-7867.

[6] Z. Lu, G. B. Hammond, B. Xu, *Acc. Chem. Res.*, **2019**, *52*, 1275-1288.

[7] M. Jia, M. Bandini, *ACS Catal.*, **2015**, *5*, 1638-1652.

[8] a) C. H. Gammons, Y. Yu, A. E. Williams-Jones, *Geochim. Cosmo. Acta*, **1997**, *61*, 1971-1983; b) J.-C. Chambron, V. Heitz, J.-P. Sauvage, *New J. Chem.*, **1997**, *21*, 237−240; c) S. Eustis, M. A. El-Sayed, *J. Phys. Chem. B*, **2006**, *110*, 14014−14019; d) G. Bergamini, P. Ceroni, V. Balzani, M. Gingras, J.-M. Raimundo, V. Morandi, P. G. Merli, *Chem. Commun.*, **2007**, 4167-4169; e) C. Mongin, I. Pianet, G. Jonusauskas, D. M. Bassani, B. Bibal, *ACS Catal.*, **2015**, *5*, 380-387; f) D. Mendoza-Espinosa, D. Rendon-Nava, A. Alvarez-Hernandez, D. Angeles-Beltran, G. E. Negron-Silva, O. R. Suarez-Castillo, *Chem.–Asian. J.*, **2017**, *12*, 203-207.

[9] M. Kumar, J. Jasinski, G. B. Hammond, B. Xu, *Chem.–Eur. J.*, **2014**, *20*, 3113−3119.

[10] Due to rapid reaction times after optimization, gold catalysis under flow chemistry is limiting the deactivation effects.

[11] a) R. Oda, S. J. Candau, I. Huc, *Angew. Chem. Int. Ed*., **1998**, *37*, 2689-2691; b) R. Oda, I. Huc, M. Schmutz, S. J. Candau, F. C. MacKintosh, *Nature*, **1999**, *399*, 566-569; c) K. Sugiyasu, S.-I. Tamaru, M. Takeuchi, D. Berthier, I. Huc, R. Oda, S. Shinkai, *Chem. Commun.*, **2002**, 1212-1213.

[12] J. Cheng, G. Saux, J. Gao, T. Buffeteau, Y. Battie, P. Barois, V. Ponsinet, M. H. Delville, O. Ersen, E. Pouget, R. Oda, *ACS Nano*, **2017**, *11*, 3806-3818.

[13] M. Attoui, E. Pouget, R. Oda, D. Talaga, G. Bourdon, T. Buffeteau, S. Nlate, *Chem.–Eur. J.*, **2018**, *24*, 11344-11353.

[14] A. Scalabre, A. Sastre-Santos, D. M. Bassani, R. Oda, *J. Phys. Chem. C,* DOI : 10.1021/acs.jpcc.0c06847.

[15] For examples of chiroptical 3D ensembles, see: Y. Luo, C. Chi, M. L. Jiang, R. P. Li, S. Zu, Y. Li, Z. Y. Fang, *Adv. Optical Mater.*, **2017**, *5*, 1700040-1700058.

[16] S. Tasan, O. Zava, B. Bertrand, C. Bernhard, C. Goze, M. Picquet, P. Gendre, P. Harvey, F. Denat, A. Casini, E. Bodio, *Dalton Trans*., **2013**, *42*, 6102-6109.

[17] a) J. P. Weyrauch, A. Schuster, T. Hengst, S. Schetter, A. Littmann, M. Rudolph, M. Hamzic, J. Visus, F. Rominger, W. Frey, J. W. Bats, A. S. K. Hashmi, *Chem.–Eur. J.*, **2010**, *16*, 956-963; b) Z. Cao, D. M. Bassani, B. Bibal, *Chem.–Eur. J.*, **2018**, *24*, 18779-18787.

[18] a) C. Nieto-Oberhuber, M. Paz Munoz, S. Lopez, E. Jimenez-Nunez, C. Nevado, E. Herrero-Gomez, M. Raducan, A. M. Echavarren, *Chem –Eur. J.*, **2006**, *12*, 1677-1693; b) M. Schelwies, R. Moser, A. L. Dempwolff, F. Rominge , G. Helmchen, *Chem.–Eur. J.*, **2009**, *15*, 10888-10900; c) W. Cao, B. Yu, *Adv. Synth. Catal.*, **2011**, *353*, 1903-1907; d) C. Gryparis, C. Efe, C. Raptis, L. N. Lykakis, M. Stratakis, *Org. Lett.*, **2012**, *14*, 2956-2959.

[19] a) Y. Zhou, Q. J. Liu, W. F. Lv, Q. Y. Pang, R. Ben, Y. Qian, J. Zhao, *Organometallics*, **2013**, *32*, 3753-3759; b) R. E. Ebule, D. Malhotra, G. B. Hammond, B. Xu, *Adv. Synth. Catal.*, **2016**, *358*, 1478-1481; c) S. Z. Liang, J. Jasinski, G. B. Hammond, B. Xu, *Org. Lett.*, **2015**, *17*, 162-165.

[20] M. D. Aparece, P. A. Vadola, *Org. Lett.*, **2014**, *16*, 6008-6011.

[21] Phenol and naphtol derivatives are also substrates for the dearomative spirocyclization catalyzed by homogeneous gold complexes: a) T. Nemoto, N. Matsuo, Y. Hamada, *Adv. Synth. Catal*., **2014**, *356*, 2417-2421; b) W. T. Wu, R. Q. Xu, L. Zhang, S. L. You, *Chem. Sci*., **2016**, *7*, 3427-3431.

[22] For this reaction under homogeneous conditions, silver triflate was an efficient chloride scavenger compared to NaOTf, KOTf and NaBArF (30 mol%) which led to no conversion.

[23] W. Zi, F. D. Toste, *Chem. Soc. Rev*., **2016**, *45*, 4567-4589

[24] A. K. Clarke, M. J. James, P. O'Brien, R. K. Taylor, W. P. Unsworth, *Angew. Chem. Int. Ed*., **2016**, *55*, 13798-13802.

[25] For a few reports of gold complexes grafted on support to avoid the degradation of supported ligand before coordination, see references 3f, 4a, 4c, 4f and 5d.

[26] a) C. M. Cobley, S. E. Skrabalak, D. J. Campbell, Y. Xia, *Plasmonics*, **2009**, *4*, 171-179; b) P. K. Jain, I. H. El-Sayed, M. A. El-Sayed, *Nano Today*, **2007**, *2*, 18-29.

[27] a) J. A. Gladysz, *Pure Appl. Chem*., **2001**, *73*, 1319-1324; (b) S. Hübner, J. G. de Vries, V. Farina, *Adv. Synth. Catal*., **2016**, *358*, 3-25.